DC protection coordination for multi-terminal HB-MMC-based HVDC grids

Niaki, Seyed Hassan Ashrafi; Chen, Zhe; Bak-Jensen, Birgitte; Sharifabadi, Kamran; Liu, Zhou; Hu, Shuju

Published in:
IET Renewable Power Generation

DOI (link to publication from Publisher):
10.1049/rpg2.12903

Publication date:
2024

Document Version
Publisher's PDF, also known as Version of record

Received: 7 June 2023 | Revised: 28 October 2023 | Accepted: 27 November 2023

IET Renewable Power Generation

DOI: 10.1049/rpg2.12903

The Institution of Engineering and Technology WILEY

ORIGINAL RESEARCH

DC protection coordination for multi-terminal HB-MMC-based HVDC grids

Seyed Hassan Ashrafi Niaki[1] | **Zhe Chen**[1] | **Birgitte Bak-Jensen**[1] | **Kamran Sharifabadi**[2] | **Zhou Liu**[3] | **Shuju Hu**[4]

[1]Department of Energy Technology, Aalborg University, Aalborg, Denmark

[2]Equinor ASA, Fornebu, Norway

[3]Siemens Gamesa Renewable Energy A/S, Copenhagen, Denmark

[4]Chinese Academy of Sciences, Beijing, China

Correspondence
Seyed Hassan Ashrafi Niaki, Department of Energy Technology, Aalborg University, Aalborg, Denmark.
Email: shani@et.aau.dk

Funding information
Sino-Danish Center for Education and Research (SDC), University of Chinese Academy of Sciences

Abstract

Fast progress of High Voltage Direct Current (HVDC) technology has been considerable over the past decades. Emerging Modular Multilevel Converter (MMC) provides power systems with promising solutions to integrate large-scale renewable energy sources, as well as multiple asynchronous power grids. Consequently, implementation of a multi-terminal HVDC transmission system has been easier using MMC converters. However, protection of multi-terminal MMC-based HVDC grids under DC fault conditions is a challenge for the industry. This study sheds light on concept of system-level DC protection coordination for multi-terminal HVDC grids. Although, there are different protection methods for HVDC transmission systems including multi-terminal ones, there are no well-defined protection coordination strategies for transmission links protection and belonging HVDC converters under DC fault conditions. The proposed protection coordination prevents unnecessary tripping of MMCs in the multi-area HVDC grids and supports the system with minimum effect on healthy parts. For the first time, different HVDC Converter Tripping (HCT) profiles are presented based on a fully selective protection strategy and their characteristics are discussed comprehensively. Simulation results demonstrate the effectiveness of the proposed strategy for multi-terminal MMC-based HVDC grids. The proposed coordination can be applied to DC grid code requirements of meshed HVDC grids in the future.

1 | INTRODUCTION

HVDC systems are cost-effective solutions for long and bulk power transmission, for example, offshore wind farms [1]. HVDC grids provide the system with flexible controllability and low power loss compared to HVAC grids [2]. HVDC technology based on Voltage Source Converters (VSC) is an attractive option for multiple infeed of HVDC grids and creation of multi-terminal DC networks. Independent control of active and reactive powers and bidirectional power flow are some fascinating features of VSC-HVDC grids [3]. Besides, MMC converters as a new generation of VSC converters made the way easier by offering more technical and economical benefits [4]. For instance, the MMC operates with a low switching frequency, which considerably reduces converter power loss. Also, it may not be necessary to use harmonic filters, as there is a negligible amount of harmonics generated on AC side. Recently, the number of multi-terminal HVDC projects in the world has rapidly increased. The world's first multi-terminal VSC-HVDC system is the Nan'ao ± 160 kV HVDC grid [5]. The three-terminal Nan'ao grid uses the Half Bridge (HB) MMC topology as its HVDC converters. The Zhangbei project is another multi-terminal HVDC grid which has been in operation in China with four ± 500 kV DC terminals [6]. Moreover, the Zhoushan ± 200 kV system is the first five-terminal MMC-based HVDC grid in the world [7]. Almost, all multi-terminal HVDC projects utilizing HB-MMCs for energy conversion.

While there are lots of protection studies on fault detection and location methods in multi-terminal HVDC grids, there is a lack of sufficient research into DC protection coordination of

MMC-based HVDC grids [8, 9]. On the other hand, the only requirement in the existing grid code documents, is that DC fault should be interrupted and DC grid should be recovered as soon as possible [10, 11]. With regard to the rapid growth of DC networks including multi-terminal HVDC grids, there should be more advanced grid codes to get the most benefits of the system under DC fault condition [12]. However, there is no efficient approach on how to have a coordinated protection for the system components including the HVDC transmission links and converters considering fault location and severity.

In a multi-terminal VSC-HVDC system, a VSC converter is usually connected to more than one transmission link. Disconnection of a VSC under DC fault condition means power interruption in all links connected to the VSC including healthy links. To have a minimum effect on healthy links and areas in multi-terminal HVDC grids, the MMCs should stay connected to the grid even under DC fault condition, if it is possible. Although, the MMC is usually blocked under DC fault conditions, it is still connected to the grid via anti-parallel diodes. This continuous connection can also improve DC system stability [13]. It can also prevent re-energization trouble of the HVDC grid by avoiding unnecessary disconnection. On the contrary, it is necessary to disconnect the MMC when it is needed to stop fault current contribution from the AC grid. For the time being, there is no systematic coordination strategy for determining whether and when an MMC should stay connected or should be disconnected under DC fault situations in multi-terminal HVDC grids with multiple MMCs. Therefore, it is vital to investigate and define a system-level protection coordination for multi-terminal MMC-based HVDC grids. Such a protection strategy can coordinate between DC link protection via DC Circuit Breakers (DCCB) and MMC converters. It can also be applicable to future DC grid codes for protection requirements.

This study presents an effective protection coordination between DCCBs as DC link protection and HB-MMC converters in multi-terminal HVDC grids under DC fault conditions. DCCBs tripping coordination considering Fault-Ride-Through (FRT) scenario assigned to MMC converters is investigated in the study. The proposed coordination not only prevents unnecessary disconnection of the MMC, but also determines when it is needed to disconnect the MMC. In this regard, an HCT profile is proposed based on DC voltage and its parameters are analyzed in this paper. Characteristics of the HCT profile are discussed based on different FRT scenarios and link protection speed. Different HCT profiles are applied to MMCs of a multi-terminal HVDC grid based on the converters' positions to fault location. The study discusses a coordinated protection approach using the HCT profiles assigned to local and remote MMCs in HVDC grids. Moreover, an analytic method is presented to calculate possible DC voltage fluctuations and sags during a DC fault, to accurately set parameters of the proposed HCT profiles. The proposed protection coordination has been evaluated using multi-terminal HVDC grids with different types of DCCBs including hybrid and mechanical ones.

This paper is organized as follows: concept of protection coordination and FRT scenarios in MMC-HVDC grids are presented in Section 2. Section 3 comprehensively describes the proposed protection coordination for multi-terminal HB-MMC-based HVDC grids. HVDC test system and simulation results are discussed in Section 4. A comparative study regarding different HCT profiles and their coordination and correlation with the DCCBs is presented in Section 5. Finally, conclusions are drawn in Section 6.

2 | PROTECTION COORDINATION AND FRT SCENARIOS IN MMC-HVDC SYSTEMS: A NEW ATTEMPT FOR DC GRID CODE

HVDC transmission system has a very low impedance compared to HVAC transmission system. Thus, magnitude of current signal suddenly increases immediately after a DC fault happens [14]. This severe current rising can be harmful to power semiconductors in MMCs. Therefore, the MMC will immediately be blocked based on converter over-current protection. However, it is still connected to main grid through freewheel diodes and contributes to the DC fault current [15]. Consequently, there should be a protection coordination to have an effective and appropriate way of tripping for DC links and MMCs during a DC fault. This is one of the main issues that the study is focused on. On the other hand, with rapid growth of the multi-terminal and meshed HVDC systems, DC networks may be a backbone grid for future power systems [16]. In addition to AC grid point of view, HVDC grids should be also addressed from DC grid point of view in future grid codes [22]. This study can also help to define system-level protection requirements for future DC grid codes.

Although, an MMC is rapidly blocked under DC fault conditions based on the converter over-current protection, it is not disconnected from the grid yet. Therefore, it is vital to have a coordinated way of tripping for all MMCs connected to the DC links in the multi-terminal HVDC grids. The protection coordination proposed in this study determines when an MMC is allowed to be disconnected from the grid, depending on the MMC's position to the fault point and the characteristics of the DCCBs. For example, suppose that a DC fault happens in link12 of the four-terminal MMC-HVDC grid shown in Figure 1.

Tripping time and blocking time of MMC1 should be different from the ones of MMC3, as they have different positions in the grid to the fault point. In this case, the MMC1&2, which are directly connected to the faulted link, should be considered as a local (main) MMC. On the other hand, the MMC3&4, which are indirectly connected to the faulted link, should be considered as a remote (adjacent) MMC. Appropriate protection coordination can be achieved by applying specific HCT profiles to each MMC based on its position to fault point. On the other hand, a fully-selective protection strategy is needed when continuous operation of healthy DC links is concerned [17]. In this type of DC protection strategy, DCCBs are installed at both ends of each DC link in multi-terminal HVDC grids, as depicted in Figure 1. Only the faulted link is isolated in this strategy and DC power can be transferred through other links during and after DC faults. Moreover, MMC positions, whether local or remote,

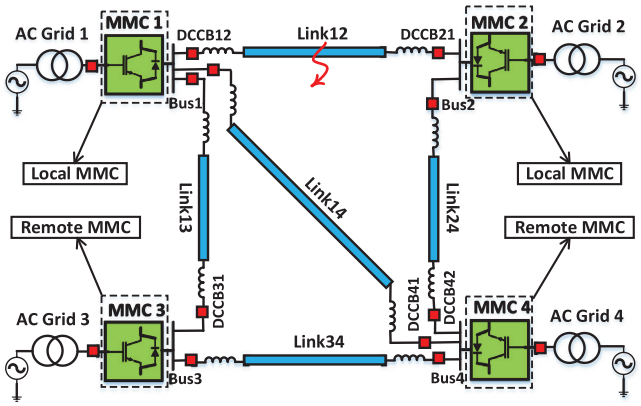

FIGURE 1 Four-terminal meshed MMC-HVDC grid

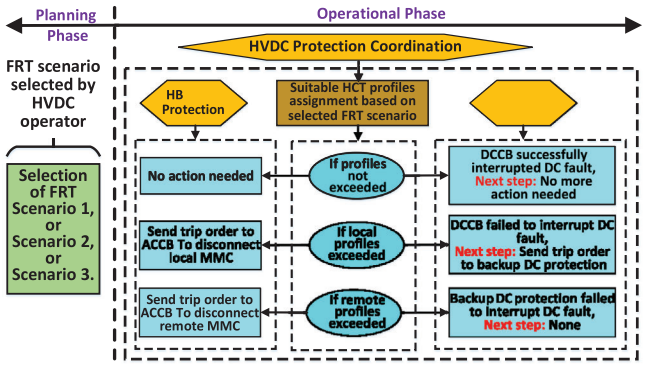

FIGURE 2 Multi-terminal HVDC coordination of HB-MMC and DC link protections based on HCT profiles and FRT scenarios

can be determined when a faulted link is detected by the DC protection system. For example, when a fault happens on link12 of the case study in Figure 1, MMC1 can continue power transmission through link13 and link 14 as long as the DC voltage does not exceed the HCT profile assigned to this MMC.

The protection coordination for HB-MMC-based HVDC grids depends on the selected FRT scenarios by the HVDC system operator. There can be three FRT scenarios in multi-terminal HB-MMC-HVDC grids as follows [18]:

- FRT scenario 1: all MMCs are forbidden to be blocked when a DC fault happens.
- FRT scenario 2: only local MMCs are allowed to be temporarily blocked, while remote MMCs are forbidden to be blocked under DC fault conditions.
- FRT scenario 3: all MMCs are allowed to be temporarily blocked under DC fault conditions.

Therefore, considering the selected FRT scenario, appropriate protection coordination should be defined, which is comprehensively discussed in the next section. Blocking MMC based on the converter over-current limitation is reflected in FRT scenarios. In each FRT scenario, DCCBs and DC inductors are selected so that the scenario requirements are fulfilled. The next step after MMC blocking is to determine an appropriate time to send a trip order to disconnect the MMC from the grid. In the proposed protection coordination, if the assigned HCT profile is exceeded, MMC should be disconnected and a trip order will be sent to ACCB on the AC side of MMC. In addition, the DCCBs of adjacent links can be ordered to open as backup protection to stop contributing to the fault current. A summary of the proposed HVDC protection coordination is shown in Figure 2.

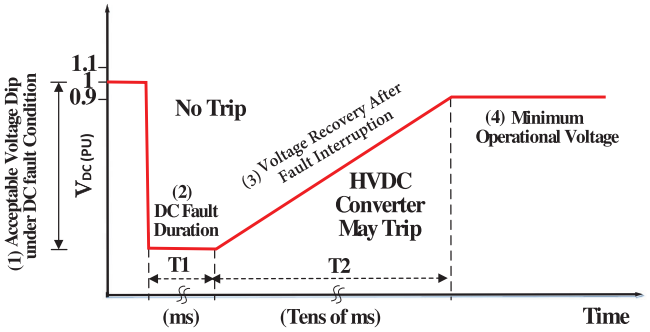

FIGURE 3 Main parameters of HVDC converter tripping (HCT) profile

3 | PROPOSED PROTECTION COORDINATION AND HCT PROFILES FOR MULTI-TERMINAL HB-MMC-HVDC GRIDS

In order to avoid unnecessary disconnection of MMC during a DC fault, a protection coordination should be defined. This coordination determines if the MMC should stay connected to the grid under the DC fault situation. The protection coordination can help the system to have the minimum possible effect on healthy parts and links of the multi-terminal HVDC grid under DC fault situations. Moreover, it can facilitate the system recovery in case of DC grid faults by providing continuous connection of the maximum possible numbers of MMCs. The proposed protection coordination for the multi-terminal HB-MMC-based HVDC grids is comprehensively investigated in this section.

3.1 | DC-voltage-based HCT profile: Main parameters, measurement points and basis

The proposed protection coordination uses a DC-voltage-against-time HCT profile to determine connection or disconnection of MMC. An abstract HCT profile with its main parameters is shown in Figure 3. If the DC voltage stays above the defined levels of the profile, the MMC should stay connected to the grid. On the contrary, if the DC voltage signal exceeds the profile, the MMC should be disconnected.

The main parameters of the HCT profile are as follows:

1. Acceptable voltage sag under DC fault condition
2. DC fault duration (T1)

3. Voltage recovery time after fault interruption (T2)
4. Minimum operational voltage

The acceptable voltage sag is the lowest limit of the HCT profile. It is related to the maximum possible voltage drop after a DC fault, discussed in the next subsection. The parameter T1 is DC fault duration, which is directly related to DC protection speed. Therefore, it depends on the time needed for the protection scheme applied to the HVDC grid to clear faults. The

DC protection time includes Fault Detection Time (FDT) plus Fault Interruption Time (FIT). Thus, the parameter T1 can be calculated as follows:

$$T_1 = k_{T1} \times \underbrace{(FDT + FIT)}_{protection\ time} \quad 1 \le k_{T1} \le 2, \tag{1}$$

where k_{T1} is the safety factor. The minimum value for T1 is equal to the DC protection time, when the safety factor is 1. However, in order to consider unpredictable time delays of the protection system, the safety factor should be selected with a value larger than 1. The parameter T2 is related to voltage recovery time after DC fault clearance. The parameter T2 can be calculated as follows:

$$T_2 = k_{T2} \times (voltage\ recovery\ time) 1 \le k_{T2} \le 2, \tag{2}$$

where k_{T2} is the safety factor for the T2 calculation. The voltage recovery time is a dynamic value depending on MMC control and the system layout of the HVDC grid. In addition, DC fault severity affects the system recovery time. For example, it is expected to have a larger recovery time in the case of Pole-to-Pole (PP) faults rather than Pole-to-Ground (PG) faults. The grid recovery time for the MMC-based HVDC grids is in the range from several tens of milliseconds to several hundreds of milliseconds [19]. However, the maximum possible value should be set for the parameter T2 in the HCT profile. The last parameter of the profile is the minimum operational voltage. This value is close to nominal DC voltage and should be set considering operational limits and voltage drop through DC links. The voltage drop through HVDC links is in the range from 3% to 5% of nominal voltage [11]. The profile parameters should be set up after a thorough review of system conditions and the time of protection scheme. Measured DC voltage for the HCT profile can be on PG basis or PP basis. The measurement points are the DC terminal of each MMC.

3.2 | Transient behavior of HVDC system under DC fault condition: Voltage sag and fluctuations

In order to present an appropriate HCT profile, it is essential to investigate transient behavior of the HVDC grid considering voltage fluctuations after a DC fault happens. Characteristics of the HCT profile including the lowest limit should be set properly. Therefore, the maximum possible value for voltage sag under DC fault situations should be analyzed and calculated. Calculation of the maximum possible value for HVDC voltage sag is not mathematically discussed in previous MMC-HVDC transient studies. Presented calculations in this subsection prove and end up minus nominal DC voltage for the lowest limit of the HCT profile. Calculations of transient voltage sags for an MMC connected to one or multiple DC links are analyzed as follows:

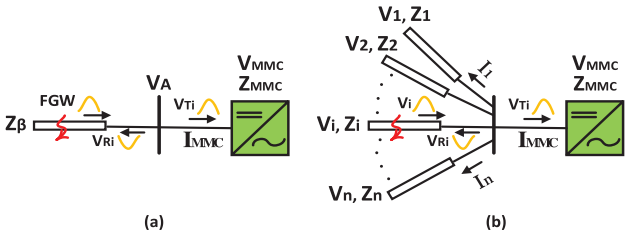

FIGURE 4 Wave propagation: (a) MMC connected to one DC link. (b) MMC connected to multiple DC links

3.2.1 | Calculation of transient voltage sags for an MMC connected to one DC link

Based on traveling wave theory, when a fault happens on a DC link, Fault-Generated Wave (FGW) moves through the faulted link toward other network points and links [20]. When the FGW reaches a point with different surge impedances, it is partly transferred and partly reflected [21]. For example, Figure 4a shows a traveling wave that comes to a DC bus (terminal A) which connects a DC link to an MMC. Transmission and reflection coefficients at the terminal A can be calculated as follows.

$$T_A = \frac{2Z_{MMC}}{Z_{MMC} + Z_\beta} = \frac{2/Z_\beta}{1/Z_\beta + 1/Z_{MMC}}, \tag{3}$$

$$R_A = \frac{Z_{MMC} - Z_\beta}{Z_{MMC} + Z_\beta}, \tag{4}$$

where Z_{MMC} is the equivalent surge impedance seen from the MMC terminal and Z_β is the surge impedance of the DC link. Similarly, the reflection coefficient at DC fault point when the reflected wave from the MMC terminal (V_{Ri}) reaches the fault point:

$$R_F = \frac{Z_{FDC} - Z_\beta}{Z_{FDC} + Z_\beta}, \tag{5}$$

where Z_{FDC} is the DC fault impedance. Under normal operational conditions, the voltage at terminal A is equal to the nominal DC pole-to-pole voltage. After a DC fault happens, the voltage of the terminal A is equal to the summation of the nominal DC voltage and sequential transmitted waves at this

terminal, as follows:

$$V_A = V_{A0} + SequentialTransmittedWaves = V_{DC} + \sum_{i=1}^{n} V_{Ti}, \quad (6)$$

where n is the number of considered transmitted waves and the summation of sequential transmitted waves can be calculated based on the transmission and reflection coefficients, neglecting damping effect, as follows:

$$\begin{aligned}\sum_{i=1}^{n} V_{Ti} &= V_{T1} + V_{T2} + V_{T3} + \cdots\cdots V_{Ti} + \cdots\cdots V_{Tn} \\ &= \underbrace{FGW \times T_A}_{V_{T1}} + \underbrace{FGW \times T_A \times (R_A R_F)}_{V_{T2}} \\ &\quad + \underbrace{FGW \times T_A \times (R_A R_F)^2}_{V_{T3}} + \cdots \\ &\quad + \underbrace{FGW \times T_A \times (R_A R_F)^{(i-1)}}_{V_{Ti}} \\ &\quad + \cdots . \underbrace{FGW \times T_A \times (R_A R_F)^{(n-1)}}_{V_{Tn}}. \end{aligned} \quad (7)$$

Equation (7) is a geometric series, which has the summation as follows:

$$\sum_{i=1}^{n} V_{Ti} = FGW \times T_A \times \left(\frac{1 - (R_A R_F)^{n+1}}{1 - R_A R_F} \right). \quad (8)$$

If time $t \to \infty$, then $n \to \infty$, consequently, the final value for the sequential transmitted waves can be expressed as follows:

$$\sum_{i=1}^{n} V_{Ti} = \frac{FGW \times T_A}{1 - R_A R_F}. \quad (9)$$

Suppose that a short-circuit PP fault with zero impedance, as a severe DC fault, happens. Based on the traveling wave theory, an FGW with magnitude is equal to DC link voltage but with reverse sign moves toward the MMC terminal A:

$$FGW = -V_{DC}, \quad (10)$$

$$\begin{cases} Z_{FDC} \approx 0 \\ Z_\beta >> Z_{FDC} \end{cases} \Rightarrow R_F = -1. \quad (11)$$

Using (9), (10), (11), the following equation can be achieved:

$$\begin{aligned}\sum_{i=1}^{n} V_{Ti} &= -\frac{V_{DC} \times T_A}{(1 - R_A R_F)} = -\frac{V_{DC} \times T_A}{(1 + R_A)} \\ &= -\frac{T_A}{(1 + R_A)} V_{DC} = -V_{DC}. \end{aligned} \quad (12)$$

Then, the final value of DC voltage at the MMC terminal A:

$$V_A = V_{A0} + \sum_{i=1}^{n} V_{Ti} = V_{DC} - V_{DC} = 0. \quad (13)$$

However, there are voltage fluctuations before the final value of DC voltage comes to zero. The maximum voltage sag happens when the first transmitted wave reaches the MMC terminal immediately after DC fault occurrence. The maximum voltage sag is important to set the lowest limit of the HCT profile. Measured DC voltage when the first transmitted wave reaches to the MMC terminal can be expressed as follows:

$$\begin{aligned} V_{AF} &= V_{A0} + V_{T1} = V_{DC} + (-V_{DC} \times T_A) \\ &= (1 - T_A) V_{DC}. \end{aligned} \quad (14)$$

Depending on the surge impedance of the link and the MMC, the DC terminal voltage can be different:

$$if \begin{cases} Z_{MMC} >> Z_\beta \Rightarrow T_A \approx 2 \Rightarrow V_{AF} \approx -V_{DC} \\ Z_{MMC} \approx Z_\beta \Rightarrow T_A \approx 1 \Rightarrow V_{AF} \approx 0 \\ Z_{MMC} << Z_\beta \Rightarrow T_A \approx 0 \Rightarrow V_{AF} \approx V_{DC} \end{cases}. \quad (15)$$

Based on (15), the minimum possible instantaneous voltage at the MMC terminal is $-V_{DC}$. Consequently, the lowest limit of the HCT profile should be set to minus nominal DC voltage.

3.2.2 | Calculation of transient voltage sags for an MMC connected to multiple DC links

Suppose that there are n DC links connected to an MMC terminal and suddenly a fault happens in link number i, as shown in Figure 4b. The main formulas for DC voltage sags and reflections are the same as what is presented in the previous part. However, the equivalent transmission and reflection coefficients will be different in this case. As all DC links and the MMC are connected to a DC bus, the following equations can be derived:

$$\begin{aligned} V_1 = V_2 = \cdots = V_{i-1} = V_{i+1} = \cdots = V_n = V_{MMC} \\ = V_{Ti} = V_i + V_{Ri}, \end{aligned} \quad (16)$$

$$I_1 + I_2 + \cdots + I_{i-1} + I_{i+1} + \cdots + I_n + I_{MMC} = I_i - I_{Ri}. \quad (17)$$

Using (16) and (17), the following formulas can be achieved:

$$V_{Ti} = \frac{2/Z_i}{\left(\frac{1}{Z_1} + \frac{1}{Z_2} + \cdots + \frac{1}{Z_i} + \cdots + \frac{1}{Z_n} + \frac{1}{Z_{MMC}} \right)} V_i, \quad (18)$$

$$V_{Ti} = T_i V_i. \quad (19)$$

Then, using (18) and (19), the transmission coefficient can be derived as follows:

$$T_i = \frac{2/Z_i}{\left(\frac{1}{Z_1} + \frac{1}{Z_2} + \cdots + \frac{1}{Z_i} + \cdots + \frac{1}{Z_n} + \frac{1}{Z_{MMC}}\right)}. \quad (20)$$

Consequently, the reflection coefficient can be expressed as follow:

$$R_i = T_i - 1 = \frac{\left(\frac{1}{Z_i} - \frac{1}{Z_1} - \frac{1}{Z_2} - \cdots - \frac{1}{Z_{i-1}} - \frac{1}{Z_{i+1}} \ldots - \frac{1}{Z_n} - \frac{1}{Z_{MMC}}\right)}{\left(\frac{1}{Z_1} + \frac{1}{Z_2} + \cdots + \frac{1}{Z_i} + \cdots + \frac{1}{Z_n} + \frac{1}{Z_{MMC}}\right)}. \quad (21)$$

Equation (20) shows that the transmission coefficient in multi-terminal HVDC system has a smaller value compared to the two-terminal system one in (3), as the denominator became larger. Therefore, probability of large voltage sag after fault happening in multi-terminal HVDC grid will be less than the two terminal ones. Also, surge impedances of DC links and MMC connected to HVDC terminal affect magnitudes of voltage sag and reflections.

3.3 | HCT profiles based on FRT scenarios of multi-terminal HB-MMC-HVDC grid and MMC position

The proposed protection coordination and profiles can be presented and regulated based on the FRT scenarios and MMC positions in multi-terminal HVDC grid as followings.

3.3.1 | Local and remote HCT profiles considering the FRT scenario 1

In this FRT scenario, all HB-MMCs including local and remote ones are prohibited from blocking under DC fault conditions. Usually, HB-MMC protection temporarily blocks the converter based on overcurrent and undervoltage thresholds [22]. The overcurrent threshold is set considering the maximum current capability of power switches. The undervoltage threshold is set considering the minimum DC voltage to keep the converter controllability. This value depends on the converter design and energy balancing control of submodule DC capacitors. Generally, the minimum voltage to keep HB-MMC controllability is based on the ratio between DC PP voltage and AC voltage of the converter transformer, so-called modulation index as follows [23]:

$$M = \frac{2\sqrt{2}V_{AC}}{\sqrt{3}V_{DC}}, \quad (22)$$

where V_{DC} and V_{AC} are DC PP voltage and AC phase-to-phase RMS voltage of the converter transformer, respectively. Then, the minimum voltage to keep HB-MMC controllability can be expressed as follows:

$$V_{\min} = M \times V_{DC}. \quad (23)$$

This value can be used as the lowest limit of the HCT profile for the FRT scenario 1, which is typically about 0.8 p.u [24]. Large DC reactors and fast DCCBs are used and sized to limit overcurrent to prevent converter blocking. Thus, these parameters are usually tuned so that the arm current does not exceed the overcurrent threshold if the DC voltage is larger than the HCT profile during T1. [18]. As a result, this approach leads to higher capital costs compared to the other FRT scenarios due to using larger DC reactors and faster DCCBs.

As shown in Figure 1, the MMC1&2 are the local MMCs when a fault happens on the link12. On the other hand, the MMC3&4 play the role of the remote MMCs in this case. This difference in the MMC's positions leads to different expected behaviors of MMCs under a DC fault condition. This different expectation can be reflected in the HCT profiles assigned to HB-MMCs. Consequently, each MMC can have two types of HCT profiles, local and remote ones, depending on its position to the fault point. The fault interruption time or the FIT parameter presented in (1) corresponds to DCCB Opening Time (DOT). Thus, the parameter T1 for the local HCT profile can be alternatively expressed as follows:

$$T_{1Local} = k_{T1} \times (FDT + DOT) 1 \le k_{T1} \le 2. \quad (24)$$

Then, the parameter T1 for the remote HCT profile can be derived as follows:

$$T_{1Remote} = T_{1Local} + CommunicationDelay + DOTofAdjacentDCCB. \quad (25)$$

When a DC fault occurs in a multi-terminal HVDC system, fully-selective protection is supposed to detect faulted link and immediately send a trip order to DCCBs assigned to faulted link. For instance, DCCB12&21 are supposed to open to isolate the faulted link12 after fault detection time as depicted in Figure 1. If the DCCBs are successful in isolating the faulted link, grid voltage recovers to nominal value and DC voltage signal will not exceed HCT profiles assigned to the local MMCs. On the contrary, if the DCCBs fail to interrupt the DC fault, DC voltage cannot recover and the local HCT profiles will be exceeded. Consequently, the local MMCs are allowed to be disconnected by AC Circuit Breaker (ACCB) at the AC side of the converter to stop the contribution of fault current from the AC side. Simultaneously, trip orders will be sent to DCCBs of adjacent links, including DCCB31&41&42, to stop contributing to fault current. However, there may be a communication delay to receive the trip orders, which is considered in (25). Therefore, a longer communication delay can lead to a longer T1 time of the remote HCT profile. If the DCCBs of the adjacent links are successful in interrupting fault current,

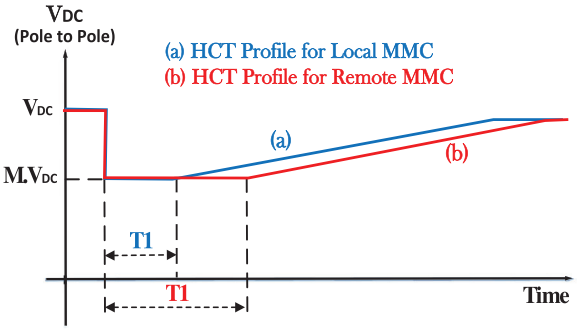

FIGURE 5 Local and remote HCT profiles for the FRT scenario 1

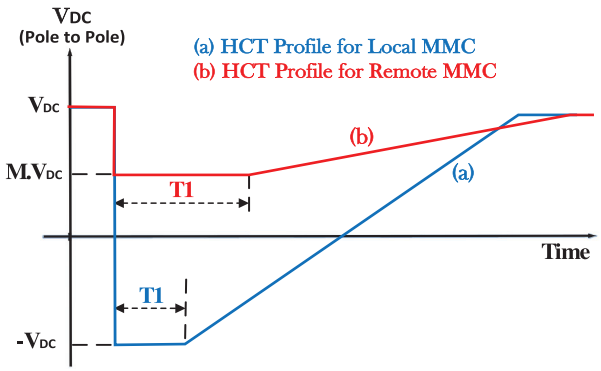

FIGURE 6 Local and remote HCT profiles for the FRT scenario 2

DC voltage recovers to nominal value before exceeding HCT profiles assigned to the remote MMCs. However, if the adjacent DCCBs also fail to do their duty as backup protection, the remote HCT profiles will be exceeded and the remote MMCs are allowed to be tripped by their ACCBs. The local and remote HCT profiles for the first scenario are depicted in Figure 5. The parameter T2 is the same for both local and remote profiles as expressed in (2).

3.3.2 | Local and remote HCT profiles considering the FRT scenario 2

While remote MMCs are forbidden to block, local MMCs are allowed to temporarily block in this FRT scenario. Therefore, the lowest limit will be different for local and remote HCT profiles. The lowest limit of the HCT profile for remote MMCs is the same as (23) presented in the previous scenario. On the contrary, this value is not limited to (23) for local MMC, as they are allowed to block. Therefore, the lowest limit of the local profiles can be set to the minimum possible voltage, that is, minus nominal value of DC voltage, as discussed in Section 3.2. Calculations of the parameters T1 and T2 are similar to what are mentioned in the previous scenario. The local and remote HCT profiles for the scenario 2 are shown in Figure 6.

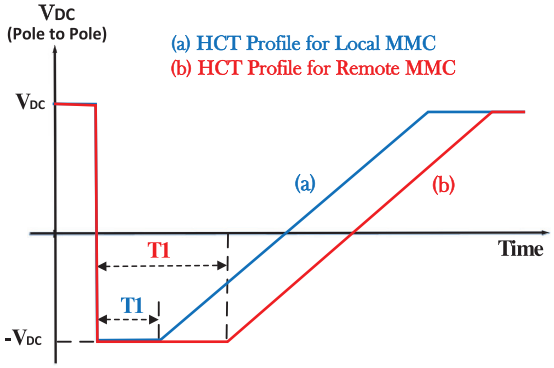

FIGURE 7 Local and remote HCT profiles for the FRT scenario 3

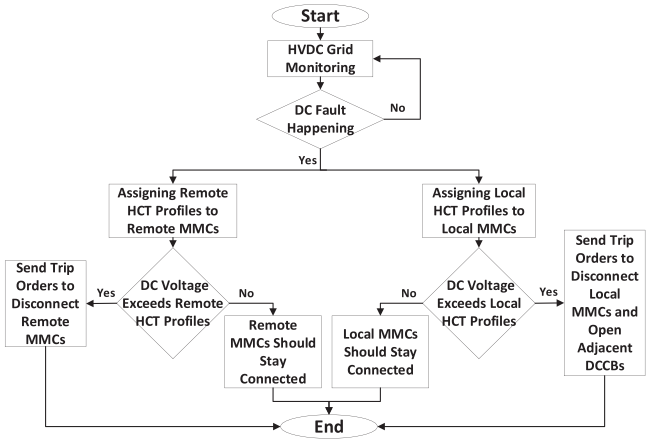

FIGURE 8 Flowchart of the proposed coordination through the HCT profiles for local and remote MMCs

3.3.3 | Local and remote HCT profiles considering the FRT scenario 3

In the third FRT scenario, all MMCs are allowed to temporarily block under fault condition. This means that the lowest limit of both local and remote profiles can be set to minus nominal DC voltage. The local and remote HCT profiles for the third scenario are depicted in Figure 7. Also, the parameters calculation of T1 and T2 are similar to the previous scenarios. Figure 8 shows a flowchart that summarizes the proposed coordination via the HCT profiles in different MMCs including the local and remote ones. As soon as a DC fault is detected, the MMCs in the grid are divided into local and remote ones depending on their position to fault location. Then, the related HCT profiles will be assigned to each MMC. Subsequent action depends on whether the DC voltage exceeds the assigned HCT profile or not.

4 | HB-MMC-BASED HVDC TEST SYSTEM AND SIMULATION RESULTS

A four-terminal meshed HVDC grid is used as the case study and performed in PSCAD/EMTDC as shown in Figure 1. The grid configuration is symmetric monopole and all HB-MMCs

are able to temporarily block under fault conditions [22]. The nominal DC voltage is ± 320 kV and the continuous converter model is used to simulate the HB-MMCs. While the MMC1 and MMC2 are integrated to offshore wind farms, the MMC3 and MMC4 are connected to AC onshore grids. The rated power of the MMC1, MMC2 and the MMC3 is 900 MW and it is 1200 MW for the MMC4. Each of the grid links has DCCBs at both ends to achieve the fully-selective protection strategy. A detailed model of DCCB is used in this case to analyze the simulation results [18]. The lengths of the link 13 and 14, the link 12 and 24, and the link34 are 400 km, 300 and 200 km, respectively. The grid links are HVDC-XLPE cables simulated using a frequency-dependent model. More details of the HVDC test system can be found in [22]. Fault detection time of the protection system is considered 2 ms for all simulation cases.

4.1 | Simulation results for the grid using hybrid DCCBs

Simulation results for the HVDC test system that uses the hybrid type of DCCB are investigated in this part. The opening time of the hybrid DCCBs is considered to be 3 ms [18]. The minimum operational voltage of the HCT profile is set to 90% of the nominal DC voltage. The values of the HCT profile parameters for the HVDC test system are given in Table A1 in the appendix, which are calculated based on the relations proposed in the previous sections. However, based on interruption time of installed DCCBs in HVDC grids and possible delays in protection system, the HCT profile parameters can be different.

Figure 9 shows DC voltages of the MMCs terminals for the case of a PP fault happening at the time 1 s in the middle of the link13 for three FRT scenarios. In this case, the MMC1&3 and the MMC2&4 are in the local and remote positions, respectively. Hybrid DCCBs assigned to the link L13 are opened to interrupt the fault. It is clear from Figures 9a and 9c that the grid voltage came back to the nominal value after some fluctuations for the FRT scenarios 1 and 3. The DCCBs were successful to isolate the faulted link on time. The DC voltages also recovered for the FRT scenario 2 as shown in Figure 9b. It can be seen from Figure 9b that DC voltages of the MMC1&3 did not exceed the local HCT profile. Therefore, these MMCs can stay connected to the grid under this fault condition.

However, their IGBTs are blocked due to severe voltage sags and the MMCs stay connected to the grid through anti-parallel diodes. On the other hand, DC voltages of the MMC2&4 did not exceed the remote HCT profile, as shown in the zoomed part of Figure 9b. Therefore, these MMCs continue their operations without blocking and this leads to a minimum effect on healthy parts under the fault condition.

Usually, PP faults at the beginning of DC links are more severe faults than the ones in the middle of links, as they have less impedance between the fault location and the converter busbar. In this test system, a PP fault case at the beginning of the link12 has been found the most severe fault with large fluctuations. Therefore, this case can be a criterion for setting the recovery time value of the HCT profiles. The results for the

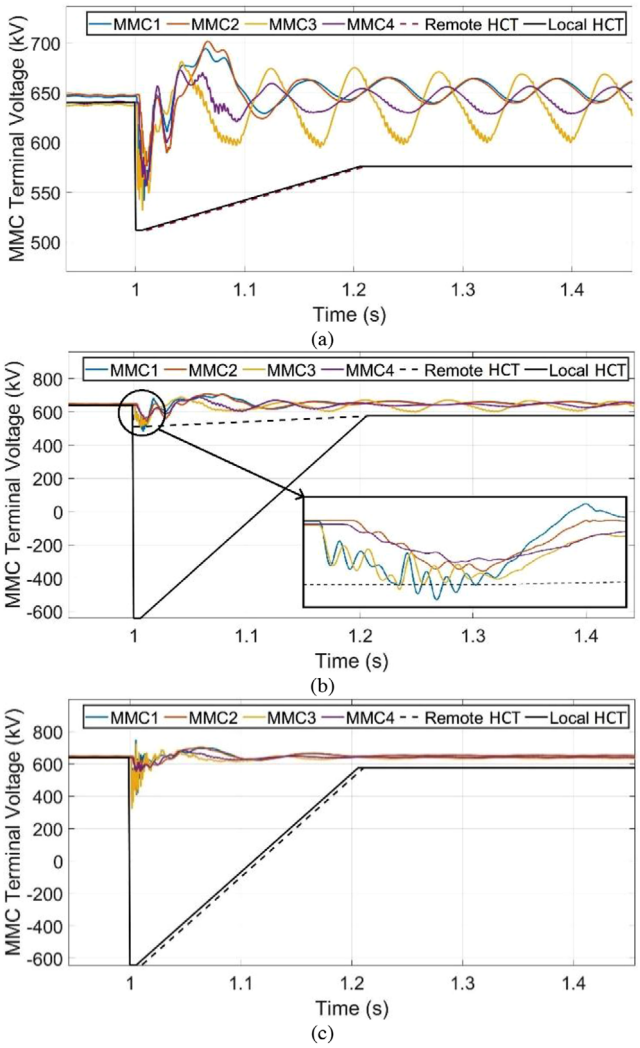

FIGURE 9 DC voltages of MMCs with local and remote HCT profiles for a PP fault case in the middle of the link13 and successful hybrid DCCB opening. (a) FRT scenario 1. (b) FRT scenario 2. (c) FRT scenario 3

case of a PP fault happening at the beginning of the link12 are shown in Figure 10. The MMC1&2 and the MMC3&4 are in the position of the local and remote, respectively. DCCB12 failed to open in the case of a fault at the beginning of the link12. Therefore, the DC voltage of the MMC1 could not come back to the nominal value. The MMC1 voltage came to zero after the local profile exceeding and consequent converter disconnection. After DCCB12 failure, DCCB31&41 are ordered to open to stop contributing to the fault current as discussed in previous sections. Then, the MMC2, MMC3 and MMC4 successfully managed to recover the grid voltage after large fluctuations. For the FRT scenario 2, DC voltages of the MMC3&4 did not exceed the remote HCT profile, as shown in the zoomed part of Figure 10b. Consequently, the MMC3&4 continued their operations without blocking under the fault condition as their DC voltages are above the remote profile. The results also demonstrate that suitable parameters are selected for the HCT profiles.

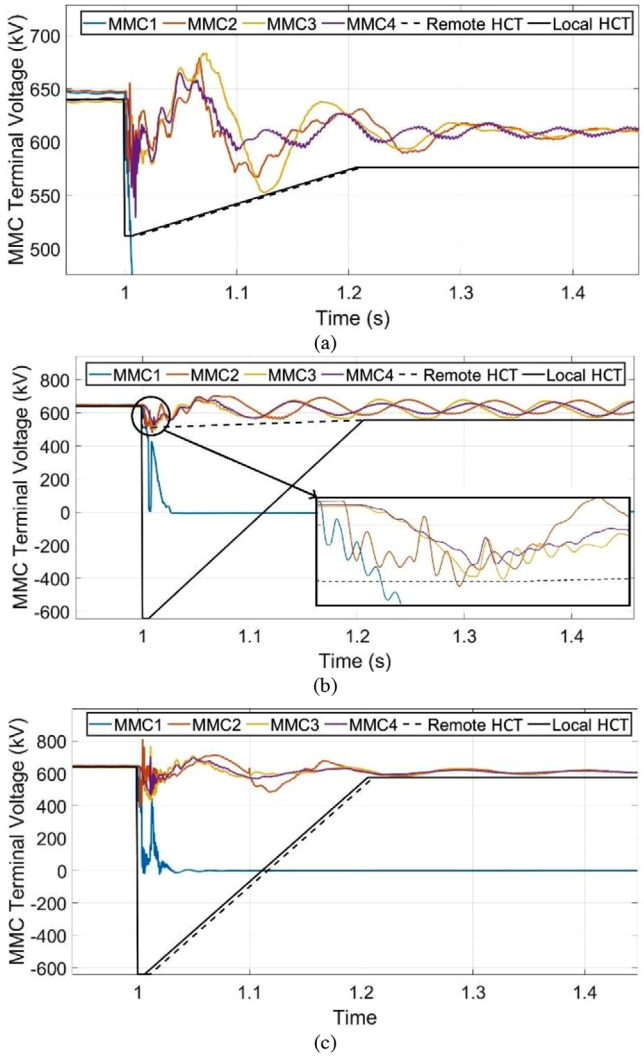

FIGURE 10 DC voltages of MMCs with local and remote HCT profiles for a PP fault case at the beginning of the link12 and failed hybrid DCCB opening. (a) FRT scenario 1. (b) FRT scenario 2. (c) FRT scenario 3

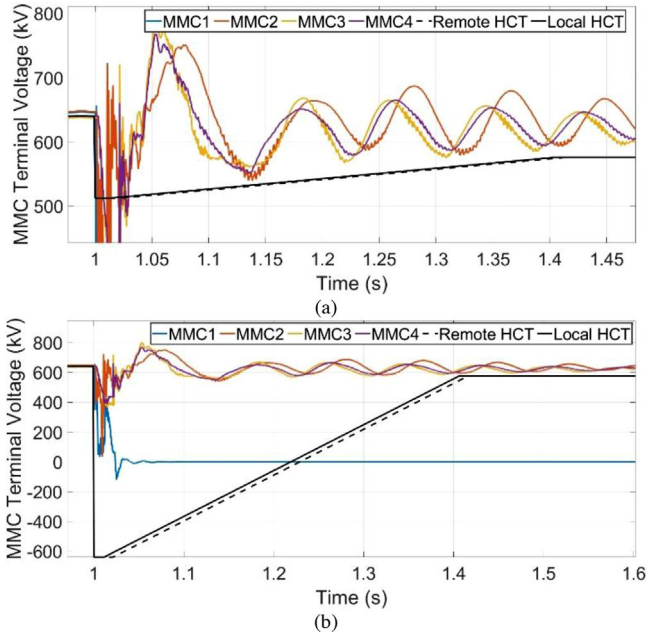

FIGURE 11 DC voltages of MMCs with local and remote HCT profiles for a PP fault case at the beginning of the link12 and failed mechanical DCCB opening. (a) FRT scenario 1. (b) FRT scenario 3

4.2 | Simulation results for the grid using mechanical DCCBs

The simulation results have also been investigated for the HVDC test system that uses the mechanical DCCBs to isolate faulted link. Opening time of the mechanical DCCBs is considered to be 8 ms [22]. Figure 11 shows DC voltages of the MMCs terminals for the case of a PP fault happening at the beginning of the link12. As shown in Figure 11b, mechanical DCCB12 assigned to the link L12 failed to interrupt the fault and DC voltage of the MMC1 came to zero after exceeding the HCT profiles. However, due to long opening time of mechanical DCCBs, large fluctuations and voltage sags happen after a severe fault as shown in Figure 11a. All DC voltages exceeded the HCT profile for the FRT scenario 1 and consequently all HB-MMCs are forced to be blocked. However, they are not supposed to be blocked for the FRT scenarios 1 and 2. Therefore, the FRT scenarios 1 and 2 cannot be applicable to the multi-terminal HVDC grid that uses mechanical DCCBs.

Consequently, only the FRT scenario 3 can be applicable in this case. For this FRT scenario, DC voltages of the MMC2, MMC3 and MMC4 have been successfully recovered to the nominal value as depicted in Figure 11b. As expected, the longer interruption time of mechanical DCCB leads to a longer recovery time. Therefore, the recovery time was longer compared to the case using the hybrid DCCBs. As depicted in Figure 11, suitable recovery time (T2) for the HCT profile has been found to be 400 ms, while it was 200 ms for the system using hybrid DCCBs.

4.3 | The impact of noise and various fault resistances on the results

To investigate the impact of noise on the proposed protection coordination, measured DC voltages are contaminated with white Gaussian noise. The results with different Signal to Noise Ratios (SNRs) are shown in Figure 12. Figure 12a depicts the results for the case of a PP fault at the middle of the link12 when the measured signals are distorted via a noise with an SNR of 40 dB. Similar to the case shown in Figure 10a, the DCCB12 failed to interrupt the DC fault. All MMC voltages except the MMC1 voltage could successfully return to the nominal value as expected. Also, Figure 12b shows the results related to the noise with an SNR of 10 dB. Like the previous case, the outputs came out as they were expected. Therefore, the distorted signals with noises could not affect the performance of the protection coordination and the HCT status significantly.

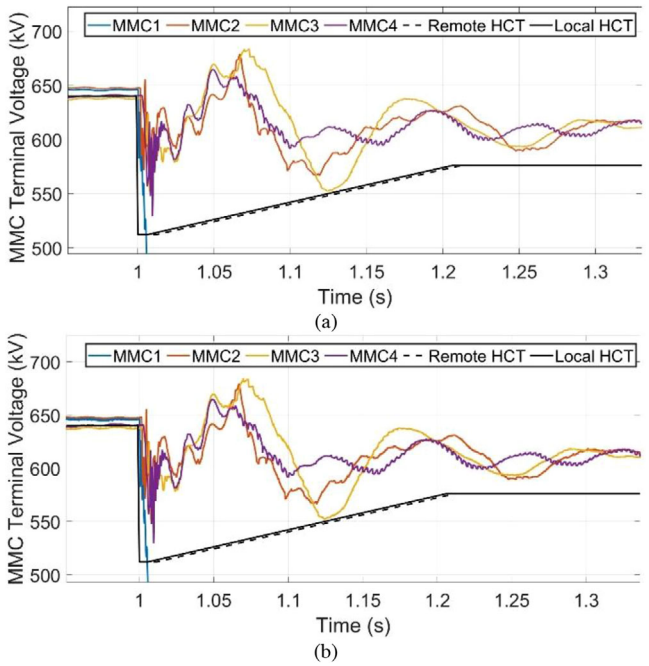

FIGURE 12 DC voltages of MMCs with local and remote HCT profiles for a PP fault case on the link12 with the first FRT scenario under noisy conditions. (a) SNR of 40 dB. (b) SNR of 10 dB

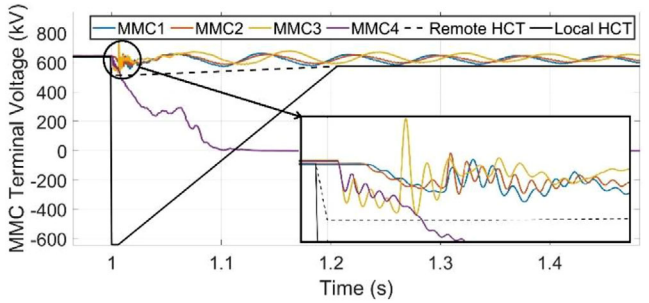

FIGURE 13 DC voltages of MMCs with local and remote HCT profiles for a PP fault case with 10 Ω resistance on the link12 when the FRT scenario 2 is applied

On the other hand, some cases have been studied for the PP faults with different fault resistances rather than zero. For example, the results of a case with a fault resistance of 10Ω with the FRT scenario 2 are shown in Figure 13. As the DCCB12 failed to interrupt the fault, the MMC1 voltage has finally come to zero. However, other MMC voltages could come back to the nominal value. Regarding the applied FRT scenario, the voltages of MMC1 and MMC2 are allowed to be blocked and consequently exceed the remote HCT profile. However, the voltage at the MMC2 terminal didn't exceed the remote HCT profile due to the high value of the fault resistance. Also, Figure 14 shows the results of the case with a fault resistance of 100Ω with the FRT scenario 2 applied. The outcomes show that the protection coordination doesn't not have difficulty with the cases with higher fault resistances.

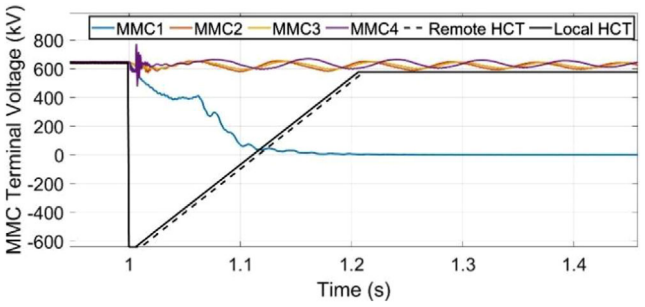

FIGURE 14 DC voltages of MMCs with local and remote HCT profiles for a PP fault case with 100 Ω resistance on the link12 when the FRT scenario 3 is applied

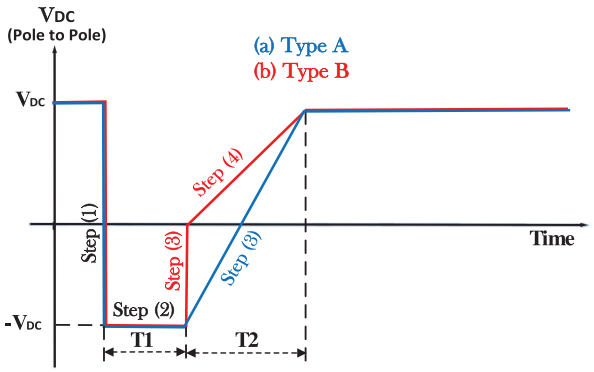

FIGURE 15 Potential HCT profiles: type A and type B

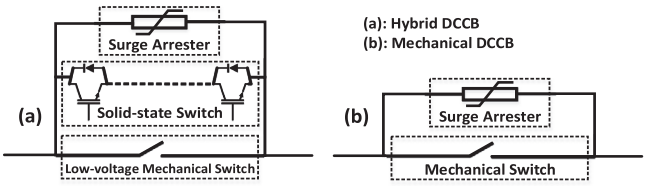

FIGURE 16 Typical topologies of hybrid and mechanical DCCBs

5 | OTHER POTENTIAL HCT PROFILES AND TEST RESULTS

HCT profiles can be classified into different types based on the profile steps and characteristics. Two types of HCT profiles, named type A and B are shown in Figure 15. The type A profile is the same depicted in Figure 3. The type B includes one step more than the type A. As it can be seen, number of the profile steps for the type A and B are three and four, respectively. However, the parameters of T1 and T2 are the same for these profiles. The profile B is more conservative than the profile A. Thus, a failure in DC link protection or the voltage recovery stage can be recognized sooner by the profile B rather than the profile A.

In order to achieve a more effective HCT profile, investigation and accurate understanding of DC fault interruption by DCCBs are necessary. Typical topologies of hybrid and mechanical DCCBs are shown in Figure 16 [25, 26]. Interruption time

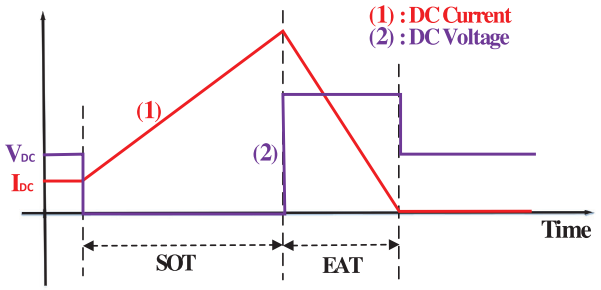

FIGURE 17 The main stages of fault current interruption by mechanical and hybrid DCCBs

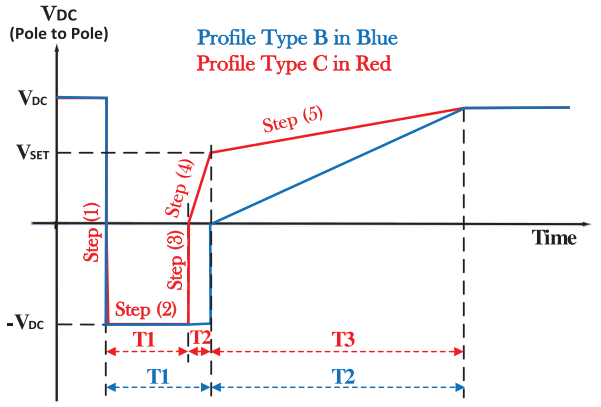

FIGURE 18 The type C of HCT profile in comparison to the type B

of DC fault current by mechanical DCCB includes two stages [25]:

1. Switch Opening Time (SOT): Mechanical switch opening time.
2. Energy Absorption Time (EAT): Surge arrester conduction time.

Similarly, the interruption time of fault current by hybrid DCCB can be divided as follows [26]:

1. Switch Opening Time (SOT): Low-voltage mechanical switch time + Solid-state switch time.
2. Energy Absorption Time (EAT): Surge arrester conduction time.

The main stages of fault current interruption by two popular types of DCCB including hybrid and mechanical ones are depicted in Figure 17. As it can be seen from Figure 17, immediately after the first stage (SOT), voltage of DC link comes back to almost nominal value [27, 28]. This feature can be used to define a developed type of HCT profile, named Type C. The step four in the profile B can be divided into two steps in the profile C as depicted in Figure 18. The profile C is the strictest and the most conservative HCT profile that can recognize a failure in protection or system recovery sooner than the type A and B. However, its parameters should be set carefully to prevent mistakenly exceeding the profile in case of successful fault interruption and system recovery. The parameters of the profile C can be expressed as follows:

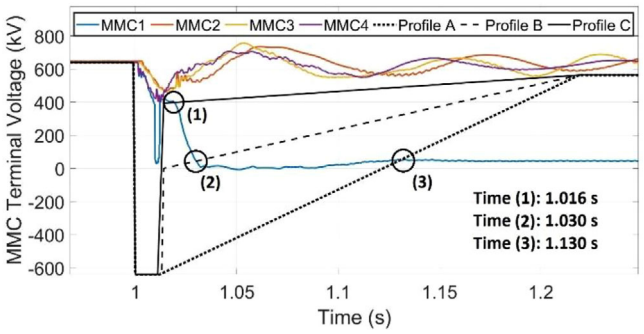

FIGURE 19 DC voltages and comparison of different types of HCT profiles for a PP fault case in the middle of the link14 and failed mechanical DCCB opening

$$\begin{cases} T_1 = k_{T1} \times (FDT + SOT) 1 \le k_{T1} \le 2 \\ T_2 = EAT \\ T_3 = k_{T3} \times (\textit{voltage recovery time}) 1 \le k_{T3} \le 2 \end{cases}, \tag{26}$$

$$V_{SET} = k_{SET} \times V_{DCnonimal} 0 < k_{SET} < 0.8, \tag{27}$$

where V_{SET} is the maximum value of the step four in the profile as shown in Figure 18. A summary of comparison of different HCT profiles is given in Table 1.

A comparative result for different types of the HCT profiles is shown in Figure 19. The DCCB14 failed to open in case of PP fault happening in the link14. Therefore, the MMC1 voltage exceeded different HCT profiles in different times. For example, it takes 16 ms for the voltage signal to exceed the profile type C after fault occurrence. While, it is 30 and 130 ms for the profile type B and type A, respectively. Thus, the profile type C can find the right situation for the converter disconnection sooner than the other types. Moreover, the profile type B can have a better performance compared to the type A, as depicted in Figure 19. Details of the parameters for the HCT profiles B and C are given inTable A2 in the appendix.

6 | CONCLUSIONS

This study presented a new protection coordination for multi-terminal HB-MMC-based HVDC grids under DC fault conditions. This coordination strategy determines if an MMC should stay connected or should be disconnected under fault conditions, based on the MMC position, defined HCT profiles and the operation of the DCCBs. The proposed coordination prevents unnecessary tripping of the MMC and reduces power outages in healthy areas of the HVDC grid. Also, it determines the appropriate time to disconnect the MMC to stop contributing to the fault current. The proposed protection coordination can be used in future DC grid codes that define the protection requirements. Different parameters of HCT profiles have been

TABLE 1 Comparison of different types OF HCT profiles

HCT profile type	Profile parameters			Strictness	Step no.
	T1	T2	T3		
A	$k_{T1} \times (FDT + DOT)$	Recovery time	–	Low	3
B	$k_{T1} \times (FDT + DOT)$	Recovery time	–	Medium	4
C	$k_{T1} \times (FDT + SOT)$	EAT	Recovery time	High	5

defined and their characteristics have been discussed. Analytical approaches have been presented to calculate the parameters of the HCT profiles including the maximum voltage sag after DC fault occurrence. Because of different DCCBs and FRT scenarios, suitable values for the parameters of the HCT profile can be different. Moreover, different potential HCT profiles have been discussed using a comparative study.

The simulation results demonstrate that the proposed coordination can be applied to HB-MMC-based HVDC grids for all FRT scenarios using hybrid DCCBs. The proposed coordination between MMC protection and DC link protection can provide the system with more reliable recovery and higher security for healthy parts. The coordination strategy presented in this study, not only can be applicable to HVDC grids, but it is also applicable to medium voltage DC networks. More studies on the application of the proposed protection coordination for different DC networks need to be done in future works.

AUTHOR CONTRIBUTIONS

Seyed Hassan Ashrafi Niaki: Writing—review & editing. **Zhe Chen**: Writing—review & editing. **Birgitte Bak-Jensen**: Writing—review & editing. **Kamran Sharifabadi**: Writing—review & editing. **Zhou Liu**: Writing—review & editing. **Shuju Hu**: Writing—review & editing.

ACKNOWLEDGEMENTS

This work is supported by the Sino-Danish Center for Education and Research (SDC), University of Chinese Academy of Sciences.

CONFLICT OF INTEREST STATEMENT

The authors declare no conflict of interest.

DATA AVAILABILITY STATEMENT

The data are available from the corresponding author upon reasonable request.

ORCID

Seyed Hassan Ashrafi Niaki https://orcid.org/0000-0002-5455-870X
Zhe Chen https://orcid.org/0000-0002-2919-4481

REFERENCES

1. Negra, N.B., Todorovic, J., Ackermann, T.: Loss evaluation of HVAC and HVDC transmission solutions for large offshore wind farms. Electr. Power Syst. Res. 76(11), 916–927 (2006)
2. Reidy, A., Watson, R.: Comparison of VSC based HVDC and HVAC interconnections to a large offshore wind farm. In: IEEE Power Engineering Society General Meeting. IEEE, Piscataway (2005)
3. Wang, W.Y., Barnes, M.: Power flow algorithms for Multi-terminal VSC-HVDC with droop control. IEEE Trans. Power Syst. 29(4), 1721–1730 (2014)
4. Marquardt, R.: Modular multilevel converter: An universal concept for HVDC-networks and extended DC-bus-applications. In: Proceedings of 2010 International Power Electronics Conference, pp. 502–507. IEEE, Piscataway (2010)
5. Rao, H.: Architecture of Nan'ao multi-terminal VSC-HVDC system and its multi-functional control. CSEE J. Power Energy Syst. 1(1), 9–18 (2015)
6. Hitachi-ABB.: Zhangbei, The world's first DC-grid with HVDC Light technology. https://www.hitachiabbpowergrids.com/references/hvdc/zhangbei
7. Li, Y.Y., Huang, X.M., Zhang, J., Sun, W.Z.: China upgrades capacity to the Zhoushan Islands: State Grid Corporation installs first HVDC five-terminal voltage source converter project (2017)
8. Ashrafi Niaki, S.H., Liu, Z., Chen, Z., Bak-Jensen, B., Hu, S.: Protection system of multi-terminal MMC-based HVDC grids: A survey. In: International Conference on Power Energy Systems and Applications (ICoPESA), pp. 167–177. IEEE, Piscataway (2022)
9. Xiang, W., Yang, S., Adam, G.P., Zhang, H., Zuo, W., Wen, J.: DC fault protection algorithms of MMC-HVDC grids: Fault analysis, methodologies, experimental validations, and future trends. IEEE Trans. Power Electron. 36(10), 11245–11264 (2021)
10. Nouri, B., et al.: Comparison of European Network Codes for AC- and HVDC-connected renewable energy sources. In: Proceedings of the 18th Wind Integration Workshop. IEEE, Piscataway (2019)
11. ENTSO-E TYNDP: Ten Year Network Development Plan 2014 (2014)
12. CIGRE: WG B4.56—Guidelines for the preparation of "connection agreements" or "grid codes" for multi-terminal DC schemes and DC grids (2016)
13. Meegahapola, L., Sguarezi, A., Bryantet, J.S., et al.: Power system stability with power-electronic converter interfaced renewable power generation present issues and future trends. Energies 13(13), 1–35 (2020)
14. He, Z., Hu, J., Lin, L., Chang, Y., He, Z.: Pole-to-ground fault analysis for HVDC grid based on common- and differential-mode transformation. J. Mod. Power Syst. Clean Energy 8(3), 521–530 (2020)
15. Li, C., Zhao, C., Xu, J., Ji, Y., Zhang, F., An, T.: A pole-to-pole short-circuit fault current calculation method for DC grids. IEEE Trans. Power Syst. 32(6), 4943–4953 (2017)
16. Wang, M., et al.: Review and outlook of HVDC grids as backbone of the transmission system. CSEE J. Power Energy Syst. 7(4), 797–810 (2020)
17. Leterme, W., Hertem, D.V.: Classification of Fault Clearing Strategies for HVDC Grids. Cigre, Paris (2015)
18. Abedrabbo, M., Leterme, W., Van Hertem, D.: Systematic Approach to HVDC Circuit Breaker Sizing. IEEE Trans. Power Delivery 35(1), 288–300 (2020). https://doi.org/10.1109/TPWRD.2019
19. Abedrabbo, M., et al.: Impact of DC grid contingencies on AC system stability. In: 13th IET International Conference on AC and DC Power Transmission (ACDC 2017). IET, Stevenage (2017)
20. Zou, G., Gao, H.: A traveling-wave-based amplitude integral busbar protection technique. IEEE Trans. Power Delivery 27(2), 602–609 (2012)
21. van der Merwe, H., van der Merwe, F.S.: Some features of travelling waves on cables. IEEE Trans. Power Delivery 8(3), 789–797 (1993)

22. Leterme, W., Ahmed, N., Beerten, J., Ängquist, L., Hertem, D.V., Norrga, S.: A new HVDC grid test system for HVDC grid dynamics and protection studies in EMT-type software. In: 11th IET International Conference on AC and DC Power Transmission. IET, Stevenage (2015)
23. PROMOTioN project.: Requirement recommendations to adapt and extend existing grid codes, Deliverable 2.4 (2020)
24. Zaja, M., Jovcic, D.: Coordination of mechanical DCCBs and temporary blocking of half bridge MMC. In: 15th IET International Conference on AC and DC Power Transmission (ACDC2019). IET, Stevenage (2019)
25. Barnes, M., Vilchis-Rodriguez, D.S., Pei, X., Shuttleworth, R., Cwikowski, O., Smith, A.C.: HVDC circuit breakers–A review. IEEE Access 8, 211829–211848 (2020)
26. Wang, Y., et al.: A practical DC fault ride-through method for MMC based MVDC distribution systems. IEEE Trans. Power Delivery 36(4), 2510–2519 (2021)
27. CIGRE B4/B5.59.: Protection and local control of HVDC grids. B4.B5.59 – Technical Brochure & Webinar (2018)
28. Cwikowski, O., Wickramasinghe, H.R., Konstantinou, G., Pou, J., Barnes, M., Shuttleworth, R.: Modular multilevel converter DC fault protection. IEEE Trans. Power Delivery 33(1), 291–300 (2018)

How to cite this article: Ashrafi Niaki, S.H., Chen, Z., Bak-Jensen, B., Sharifabadi, K., Liu, Z., Hu, S.: DC protection coordination for multi-terminal HB-MMC-based HVDC grids. IET Renew. Power Gener. 1–13 (2023). https://doi.org/10.1049/rpg2.12903

APPENDIX

TABLE A1 Proposed parameters of the HCT profile for the HVDC test system

	HCT profile parameters			
DCCB type	**T1Local**	**T1Remote**	**T2**	**kT1**
Hybrid	6 ms	12 ms	200 ms	1.2
Mechanical	12 ms	24 ms	400 ms	1.2

TABLE A2 Proposed parameters of the HCT profiles B and C

	HCT profile type			
	B		**C**	
Parameters	**Mech DCCB**	**Hybrid DCCB**	**Mech DCCB**	**Hybrid DCCB**
T1Local	12 ms	6 ms	10 ms	5 ms
T1Remote	24 ms	12 ms	20 ms	10 ms
T2	200 ms	100 ms	1 ms	1 ms
T3	–	–	200 ms	100 ms
kT1	1.2	1.2	1.2	1.2
kSET	–	–	0.6	0.6